Magnetism in intermediate-valence $YbAl_3$: a polarized neutron diffraction study

2000 J. Phys.: Condens. Matter 12 829

(http://iopscience.iop.org/0953-8984/12/6/307)

J. Phys.: Condens. Matter **12** (2000) 829–840. Printed in the UK PII: S0953-8984(00)06293-7

Magnetism in intermediate-valence $YbAl_3$: a polarized neutron diffraction study

A Hiess†‡§, J X Boucherle†[+], F Givord†[+], J Schweizer†, E Lelièvre-Berna§, F Tasset§, B Gillon‖ and P C Canfield¶

† Département de Recherche Fondamentale sur la Matière Condensée, CEA/Grenoble, F-38054 Grenoble Cédex 9, France
‡ European Commission, JRC, Institute for Transuranium Elements, Postfach 2340, D-76125 Karlsruhe, Germany
§ Institut Laue–Langevin, BP 156, F-38042 Grenoble Cédex 9, France
‖ Laboratoire Léon Brillouin, CEA/Saclay, F-91191 Gif-sur-Yvette Cédex, France
¶ Ames Laboratory, Iowa State University, Ames, IA 50011, USA

Received 22 July 1999, in final form 19 November 1999

Abstract. Polarized neutron diffraction experiments on $YbAl_3$ have revealed the following: (i) a field-induced magnetic moment on the ytterbium site only, which is well described by a Yb^{3+} free-ion form factor; (ii) a second maximum at $T \approx 15$ K in the temperature dependence of the localized magnetic moment in addition to the well-known maximum at $T = 130$ K; and (iii) a small temperature-independent positive conduction electron polarization. The possible microscopic origin of those observations is discussed. A comparison with the isostructural intermediate-valence compound $CeSn_3$ reveals important differences which increase our understanding of the ground state in those compounds.

1. Introduction

Intermetallic compounds containing the rare-earth element ytterbium show unusual properties like Kondo behaviour or intermediate valence as observed also in cerium and uranium intermetallic compounds [1]. The proximity of the energy level of the 4f electrons and the Fermi level results in a hybridization of the 4f electrons with the conduction electrons. Depending on the strength of the hybridization, Kondo or intermediate-valence behaviour is observed.

The intermetallic compound $YbAl_3$ has been investigated for many years. $YbAl_3$ crystallizes in the cubic $AuCu_3$ structure. From transport, magnetic and thermodynamic properties, $YbAl_3$ may be classified as an intermediate-valence system, but with almost trivalent ions [2–7]. The almost integer valence has raised the expectation that $YbAl_3$ should show heavy-fermion behaviour. But the linear coefficient of the specific heat $\gamma = 45$ mJ K^{-2} mol^{-1} is reasonably small. However, a Kondo temperature of 400 K has been proposed [8]. Several photoemission studies have been performed to characterize the ground state [8–13]. The temperature dependence of the spectra observed by Tjeng *et al* [12] has been interpreted as Kondo resonance but recent measurements on single crystals did not confirm such a temperature dependence [8]. The magnetic excitation spectrum has been investigated with inelastic neutron scattering on powder samples [14–16] as well as on single crystals [17]. At low temperatures no magnetic excitations have been observed at small energy transfer. But for $\Delta E > 30$ meV

[+] CNRS staff.

0953-8984/00/060829+12$30.00

the magnetic intensity increases rapidly and exhibits a maximum at $\Delta E \approx 32$ meV. This suggests an energy gap of about 30 meV. The signal gets broader at higher temperatures and cannot be distinguished from a quasielastic response above $T = 130$ K.

Some time ago we reported on magnetic measurements on single crystals [18] and compared the results to those of earlier measurements on polycrystalline samples [4–7]. First, for both kinds of sample, a maximum in the temperature dependence of the magnetic susceptibility has been observed at $T = 130$ K. This maximum, as well as the observed Curie–Weiss temperature dependence at higher temperatures, are typical features of many intermediate-valence (and heavy-fermion) Ce and Yb compounds. Second, magnetic impurities can explain the observed 'rising tails' which appear in the low-field susceptibility below 25 K for the polycrystals and below 6 K for the single crystal. Finally, using the single-crystalline sample, in which the impurity concentration is very low (≈80 ppm), a second maximum—besides the one at $T = 130$ K—in the temperature dependence of the magnetic susceptibility has been directly observed at $T = 15$ K. For the polycrystalline samples this second maximum could only be noticed after subtraction of a large Curie-like impurity contribution.

Recently, we reported briefly on polarized neutron diffraction investigations on $YbAl_3$ [19] from which the following have been concluded:

(i) Only the Yb ions carry a magnetic moment.
(ii) The form factor can be best fitted by a free-ion form factor of Yb^{3+}.
(iii) The low-temperature maximum at $T = 15$ K appeared to be related to the localized 4f moment even though only four different temperatures had been measured at the time.
(iv) A temperature-independent difference between the total and the localized moment has been observed, suggesting a positive conduction electron polarization.

In this paper we review the above-mentioned experiments and describe the details of the data analysis. In addition, we present a new detailed study of the unusual temperature dependence of the localized magnetic moment. Furthermore, we here discuss for the first time the possible microscopic origin of those observations. Finally, we will compare the magnetic properties of $YbAl_3$ with those of the isostructural intermediate-valence compound $CeSn_3$.

2. Experimental details

2.1. Sample preparation

The $YbAl_3$ sample was a single crystal with a mass of $m = 0.8$ g grown from aluminium flux [20]. This method of growth is known to avoid contamination with the neighbouring $YbAl_2$ phase and to produce very pure crystals. Our crystal is identical to the one used before for the magnetization experiments [18], and similar to those used for the photoemission studies [8]. Precautions were taken to limit the contact of the sample with air to avoid oxidation. For the neutron diffraction experiments the crystal was oriented and cut into a bar of $8.5 \times 4.5 \times 2.5$ mm^3 elongated along the [1 1 0] direction.

2.2. Crystallographic studies

For crystallographic characterization of the sample, neutron experiments were performed at room temperature using the four-circle diffractometer DN4 ($\lambda = 1.176(1)$ Å) of the Siloé reactor (CEA/Grenoble). The observed value of the lattice parameter $a = 4.202(4)$ Å is consistent with the literature. The width of the reflections (FWHM ≈ 0.4 deg) is resolution limited. Due to sample size and the large Yb scattering length of 12.4 fm, the observed intensities are large. Only the special positions *a* and *c* of space group $Pm3m$ are occupied

by the Yb and Al atoms, respectively. Therefore a scale factor, the temperature factors and the extinction parameter(s) have been varied in a least-squares refinement of the observed intensities. The model of Becker and Coppens [21] has been used to correct for the extinction effects. But, the refined extinction parameter is very large, resulting for the strongest reflections in a 70% reduction of the intensities with respect to the intensities calculated from kinematical theory. For such strong extinction the resulting parameters are not necessarily physically meaningful and therefore of limited use only. Since the effect of extinction depends strongly on the wavelength, the polarized neutron experiments were performed at several shorter wavelengths to ensure a correct evaluation of the extinction effects.

2.3. Polarized neutron studies

Flipping ratios $R(h\,k\,l) = I^+/I^-$ were measured in an external magnetic field of $B = 4.65$ T applied along the [1 1 0] crystallographic axis at different temperatures and at several wavelengths using the polarized neutron diffractometers DN2 of the Siloé reactor (CEA/Grenoble), D3 of the ILL, and 5C1 of the LLB (CEA/Saclay). The experimental conditions for those measurements are summarized in table 1. As an example, we reproduce the flipping ratios measured on D3 at $T = 2$ K and $\lambda = 0.84$ Å in table 2.

Table 1. Experimental conditions for the data collection with polarized neutrons. The columns refer to the polarized neutron diffractometer used, the wavelength λ, the temperature T, and the number of flipping ratios $R(h\,k\,l) = I^+/I^-$. The absolute error in the wavelength is $\Delta\lambda < 0.01$ Å, the relative error in the temperature stability $\Delta T/T < 3\%$.

Instrument	λ (Å)	T (K)	Number of ratios R
DN2	1.21	2	28
DN2	1.21	15	28
DN2	1.21	75	16
DN2	1.21	130	28
D3	0.84	2	65
D3	0.71	2	15
D3	0.50	2	17
D3	0.50	15	8
D3	0.42	2	8
5C1	0.84	15	13
5C1	0.84	50	13
5C1	0.84	130	13
D3	0.84	5–260	1

In addition, we measured carefully the temperature dependence of the (0 0 1) Bragg reflection on D3 with polarized neutrons of $\lambda = 0.843$ Å.

Extinction effects have to be taken into account when extracting the magnetic structure factors F_M from the flipping ratios. We describe the extinction in the model of Becker and Coppens [21]. The observed reduction of intensity is described by

$$y = \frac{I}{I_0} = \left(1 + 2x + \frac{A(\Theta)x^2}{1 + B(\Theta)x}\right)^{-1/2}$$

where $A(\Theta)$ and $B(\Theta)$ are polynomial functions in $\cos 2\Theta$.

$$x = (2/3)(\lambda^3/(V^2 \sin 2\Theta))\alpha \bar{T} F^2$$

Table 2. Flipping ratios measured on D3 at $T = 2$ K and $\lambda = 0.84$ Å. Equivalent reflections have been averaged.

Reflection ($h\,k\,l$)	$\sin(\Theta)/\lambda$	R	ΔR
1 0 0	0.122	1.03346	0.00032
1 1 0	0.172	1.03378	0.00033
1 1 1	0.211	1.01030	0.00023
2 0 0	0.243	1.00918	0.00029
2 1 0	0.272	1.02902	0.00046
2 1 1	0.298	1.03052	0.00050
2 2 0	0.344	1.00809	0.00046
2 2 1	0.365	1.02742	0.00082
3 0 0	0.365	1.02865	0.00123
3 1 0	0.385	1.02697	0.00081
3 1 1	0.404	1.00793	0.00038
2 2 2	0.422	1.00770	0.00072
3 2 0	0.439	1.02151	0.00140
3 2 1	0.455	1.02177	0.00095
4 0 0	0.487	1.00690	0.00062
3 3 0	0.516	1.01831	0.00149
4 1 1	0.516	1.02051	0.00085
3 3 1	0.531	1.00610	0.00081
3 3 2	0.571	1.01658	0.00177
4 2 2	0.596	1.00576	0.00062
3 3 3	0.632	1.00510	0.00065
5 1 1	0.632	1.00490	0.00080
4 4 0	0.689	1.00319	0.00080
4 4 2	0.730	1.00357	0.00114
6 0 0	0.730	1.00326	0.00109
6 1 1	0.750	1.00936	0.00243
5 3 3	0.798	1.00211	0.00135
6 2 2	0.807	1.00387	0.00078
4 4 4	0.843	1.00269	0.00109
5 5 0	0.861	1.00638	0.00225
5 5 1	0.869	1.00138	0.00095
7 1 1	0.869	1.00346	0.00080
5 5 3	0.935	1.00319	0.00124
8 0 0	0.974	1.00251	0.00138
7 3 3	0.996	1.00326	0.00125

depends on the structure factor F, the crystal volume V, the wavelength λ, the scattering angle 2Θ, the path $\bar{T}$, and a function α describing the mosaicity of the crystal. Considering secondary extinction only and a Gaussian distribution of perfect crystalline blocks, one finds

$$\alpha_{\mathrm{G}} = \left[\left(\frac{\lambda}{r \sin(2\Theta)} \right)^2 + \frac{1}{2g^2} \right]^{-1/2} .$$

The parameter g is related by $\eta = (2\sqrt{\pi}g)^{-1}$ to the mosaicity η. Assuming the radius r of the polycrystalline blocks to be significantly larger than the wavelength λ, the first term can be ignored. In this case the extinction correction depends on the parameter g only.

Figure 1 shows graphically the importance of extinction. The magnetic structure factors F_{M} calculated from the flipping ratios are plotted as a function of the extinction parameter g. The F_{M} deduced from measurements at different wavelengths λ are consistent for

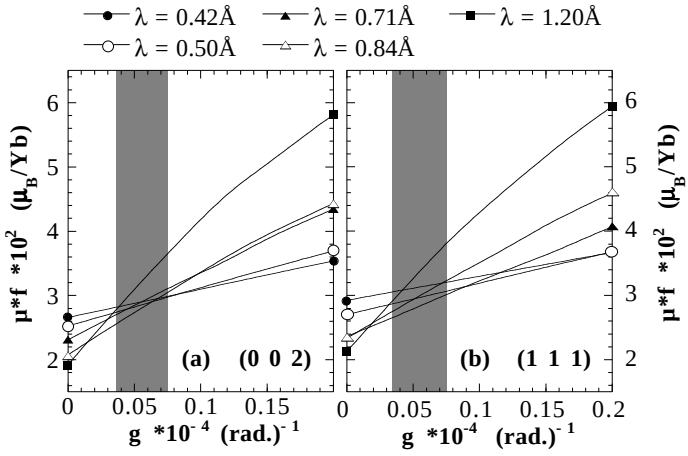

Figure 1. Magnetic structure factors as calculated from the flipping ratios measured at different wavelengths versus the extinction parameter g for the Bragg positions (a) (0 0 2) and (b) (1 1 1). Consistent magnetic structure factors are obtained for $g = 550 \pm 200$ rad^{-1}.

$g \approx 550 \pm 200$ rad^{-1}, which corresponds to a mosaicity of $\eta = 1.7' \pm 0.3'$. A non-linear variation with g has been observed only for data at $\lambda = 1.2$ Å. This suggests that a reliable extinction correction cannot be reached at this wavelength with the above-mentioned model. Data on the strong reflections measured at this wavelength have been excluded in the following data analysis. The measurements at one temperature, but obtained for different wavelengths, have been combined into one data set; the error on the deduced magnetic structure factors takes the uncertainty of the extinction correction into account.

3. Data analysis

3.1. Magnetization density

The magnetic structure factors $F_{\mathrm{M}}(q)$ are the Fourier components of the magnetization density $M(r)$ in the unit cell. We reconstructed the real-space magnetization density at $T = 2$ K from the magnetic structure factors using simple Fourier transformation as well as a two-dimensional maximum-entropy treatment. The latter is a model-free algorithm, which calculates the most probable density map of the magnetization consistent with the experimental results [22]. Loosely speaking, this procedure considers the measured magnetic structure factors with their experimental error for the reconstruction of the magnetization density, whereas simple Fourier transformation takes all unmeasured magnetic structure factors to be zero and treats the measured ones as 'exact'. Figure 2 shows the resulting projected magnetization-density maps. The spurious contours obtained in the case of Fourier transformation (figure 2(a)) outside the Yb site are due there being a finite number of measured Fourier components, and those effects disappear in the maximum-entropy treatment (figure 2(b)). Hence the two methods lead to consistent results and show that only the Yb carries an induced magnetic moment.

3.2. Form-factor analysis

For the crystal structure of $YbAl_3$ and using the fact that only the Yb carries a magnetic moment, the product of the Yb form factor and the induced magnetic moment μf can be deduced

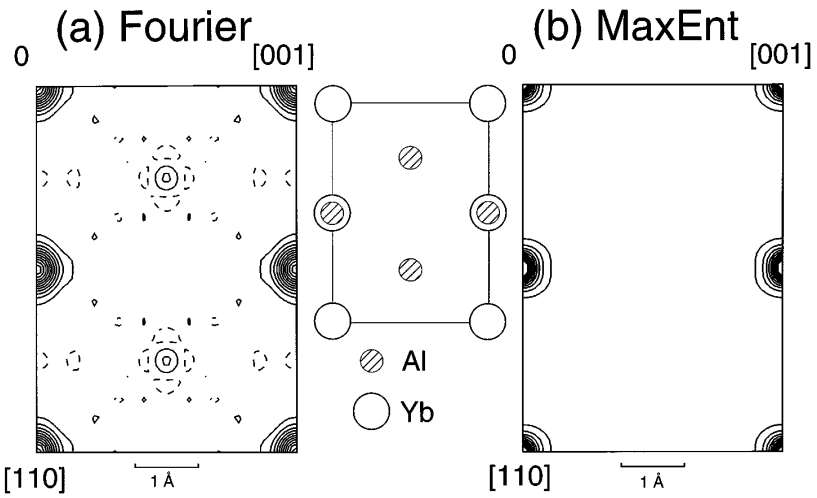

Figure 2. Projection along the $[1\,\bar{1}\,0]$ axis of the magnetization density of $YbAl_3$ at $T = 2$ K reconstructed from the magnetic structure factors with (a) simple Fourier transformation and (b) a two-dimensional maximum-entropy treatment (MaxEnt). The step between the contours is 13.3×10^{-3} μ_B Å^{-2} from -6.7 to 140×10^{-3} μ_B Å^{-2} for the Fourier map and from 6.7 to 193×10^{-3} μ_B Å^{-2} for the MaxEnt map.

from the flipping ratios R. The intermediate-valence behaviour of $YbAl_3$ might naively be described by Yb ions in divalent and trivalent states. As the electronic configuration of Yb^{2+} $S = L = J = 0$ is non-magnetic, it is reasonable to consider a trivalent configuration Yb^{3+} only for the following analysis of the Yb form factor. The dipole approximation $\mu f = \mu(\langle j_0\rangle + c_2\langle j_2\rangle)$ for a Yb^{3+} form factor has been used to fit the data at different temperatures (figure 3). For the data at $T = 2$ K the magnetic moment μ as well as the parameter c_2 have been varied. The observed value of $c_2 = 0.67 \pm 0.03$ is in agreement with the value $c_2 = 0.667$ expected in the spherical dipole approximation [23] for a Yb^{3+} free ion. As this fit of the magnetic moment might be biased by the data at small scattering angles, we excluded all reflections with $\sin(\Theta)/\lambda < 0.25$ Å^{-1} in a second refinement. The deduced magnetic moment is identical within the error bars in both refinements.

Also at higher temperatures, at which fewer reflections have been measured, the form factor is well described with a form factor of a Yb^{3+} free ion. For the final fit $c_2 = 0.667$ has been fixed to the theoretical value and only the magnetic moment has been determined at all other temperatures. The results of the fit for the induced magnetic moments at those four temperatures are summarized in table 3. The thermal variation of the induced moment localized on the Yb site is compared to that of the total magnetic moment as measured by bulk magnetization measurements on the same single crystal [18] in figure 4(a). The temperature dependence is similar and, in particular, a second maximum at $T = 15$ K besides the one at $T = 130$ K has been observed, as has already been concluded in reference [19].

This second maximum is further evidenced by the temperature dependence of the flipping ratio of the (0 0 1) Bragg reflection (figure 4(b)). $R - 1$ is a relative but direct measure for the localized moment as its observation does not depend on any fitting procedure for the form factor nor the extinction corrections.

Nevertheless, comparing the absolute values of the total moment as obtained from the magnetization measurements and the localized moment as deduced from the form factor we find that they are different: the localized moment is *smaller* than the total moment (table 3).

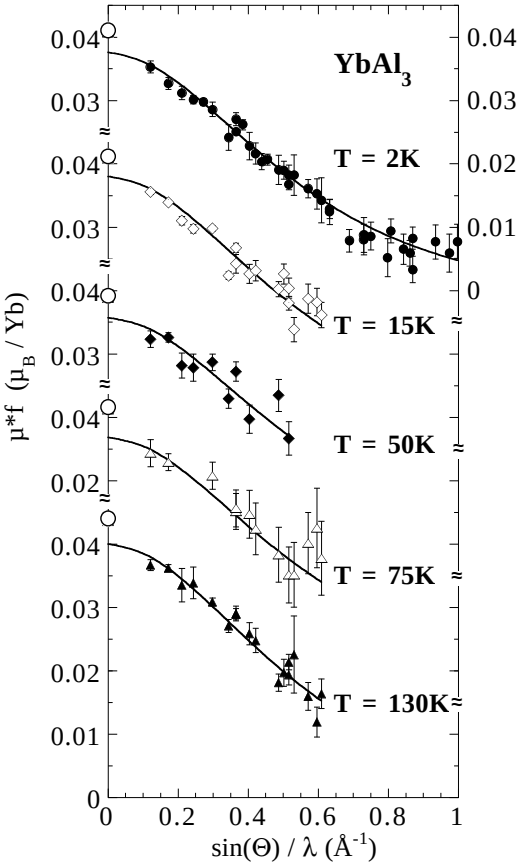

Figure 3. The ytterbium form factor at (from top to bottom) $T = 2$ K, $T = 15$ K, $T = 50$ K, $T = 75$ K and $T = 130$ K. The solid line is a fit to the Yb^{3+} free-ion form factor. The total induced moment from the magnetization measurements is shown as open circles.

Table 3. Localized and total magnetization of $YbAl_3$ as a function of temperature in an applied magnetic field of $B = 4.65$ T. The difference corresponds to the delocalized part of the magnetization and hence the conduction electron polarization (CEP).

T (K)	4f moment (10^{-3} μ_B)	Total bulk magnetization (10^{-3} μ_B)	Difference μ_{CEP} (10^{-3} μ_B)
2	37.2 (0.8)	41.0 (0.2)	3.8 (1.0)
15	37.6 (1.0)	41.2 (0.2)	3.6 (1.2)
50	35.3 (1.5)	39.2 (0.2)	3.9 (1.7)
75	36.4 (1.5)	41.5 (0.2)	5.1 (1.7)
130	40.1 (1.5)	44.2 (0.2)	4.2 (1.7)

The individual error bars at a given temperature are of the order of 30%. Having established that the temperature dependences for the total and the localized moment are similar, we deduce a temperature-independent difference of about $\mu_{CEP} = (4.0 \pm 0.6) \times 10^{-3}\ \mu_B$ by averaging over the four individual measurements. Even though this difference seems to be quite small in absolute numbers, it is experimentally significant (6 times larger than the experimental error) and corresponds to about 10% of the absolute induced moment.

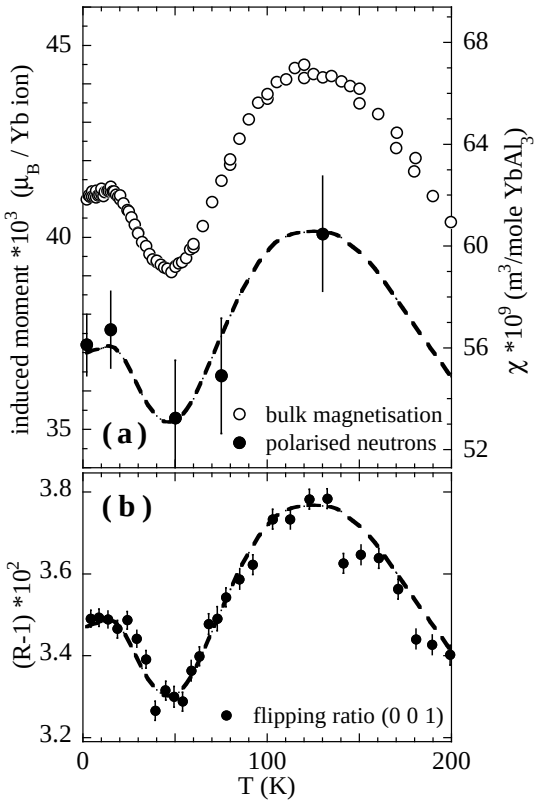

Figure 4. (a) The temperature dependence of the induced magnetic moment. The open symbols show the total moment as deduced from magnetization measurements (taken from reference [18]), the closed symbols the localized moment as deduced from the magnetic form factor measured with polarized neutron diffraction (taken from reference [19]). The error bars correspond to the absolute error in the local moment as deduced from the form-factor fit. (b) The thermal variation of the flipping ratio R measured at the (0 0 1) reflection, plotted as $R - 1 \propto \mu$. In this case the error bars correspond to the relative statistical error in the measurement. The dotted line is obtained by a vertical shift of the bulk magnetization data. The applied field of $B = 4.65$ T was identical in all measurements.

4. Discussion

4.1. Temperature dependence of the magnetic moment

The polarized neutron diffraction experiments as well as the magnetization studies performed on the same sample [18] give us information on the temperature dependence of the magnetic moment. In addition to the well-known maximum in the susceptibility at $T = 130$ K, both measurements reveal a second shallow maximum at $T = 15$ K. Below $T = 6$ K we observed a 'rising tail' in the bulk susceptibility in low applied fields only.

These rising tails are well described by a Curie-like ((C/T)-type) increase, and can be explained by the presence of either magnetic impurities or a few Yb^{3+} ions in the $YbAl_3$ lattice. At low temperatures and in high applied magnetic fields, their contribution would saturate whereas the paramagnetic magnetization of $YbAl_3$ has a linear variation with applied field. The contribution of the 'rising tail' becomes therefore negligible in higher applied

magnetic fields, and in fact, it has not been observed either in the high-field magnetization measurements or in the polarized neutron studies.

For all temperatures above 6 K, the measured magnetization increases linearly with the field [18]. The susceptibility $\chi = \partial M/\partial B = M/B$, and thus the second maximum found at $T = 15$ K is field independent. Several hypotheses can be advanced to explain the origin of this second maximum.

(i) An impurity effect as discussed to explain the 'rising tails' could also be proposed to be responsible for this second maximum. But as the polarized neutron diffraction experiments are sensitive to a periodic magnetization in the $YbAl_3$ lattice only, it can be excluded that the maximum at 15 K of the induced moment is due to a magnetic impurity phase in our sample.

(ii) Let us now imagine that a few free Yb^{3+} ions exist in the $YbAl_3$ lattice. At $T = 15$ K, the Yb^{3+} and $YbAl_3$ contributions are both linear with fields up to 5 T, which is in agreement with the observation of a field-independent susceptibility. But such a contribution would show a Curie-like thermal variation ((C/T)-like susceptibility), and it cannot lead to a local maximum in the susceptibility at $T = 15$ K.

(iii) Nevertheless, if several such magnetic Yb^{3+} ions are placed on neighbouring Yb sites their magnetic interaction can be expected to be antiferromagnetic, and this can give rise to a local short-range antiferromagnetic order. The partial alignment of the antiferromagnetically ordered moment with the applied field would result in a linearly field-dependent magnetization, and hence a field-independent susceptibility as experimentally observed and a possible maximum in the temperature variation [24]. One possible origin of such a magnetic 'cluster' is shown in figure 5: a missing Al atom changes locally (at least) the electron density of *four* neighbouring Yb ions which will be the germ of a magnetic cluster. Also other perturbations in the $YbAl_3$ lattice such as Yb^{3+} ions on an Al site or even interstitial positions could lead to magnetic clusters. No coherence between those magnetic clusters, which are statistically distributed in the mainly paramagnetic $YbAl_3$ lattice, are assumed in this model, but we cannot exclude the possibility that information on the phase of a magnetic cluster is transmitted to the neighbouring clusters. However, our polarized neutron diffraction experiments do not allow us to draw any conclusions either as to the size (correlation length) or as to the concentration of such clusters.

(iv) Finally, the second maximum that we observed in the temperature dependence of the magnetic moment could well be an intrinsic property of $YbAl_3$, especially as the

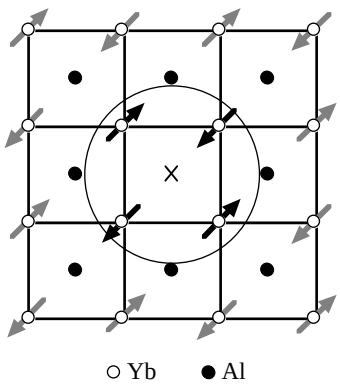

Figure 5. A possible magnetic cluster leading to a short-range magnetic order inside the $YbAl_3$ lattice.

magnetization increases linearly with the applied magnetic field and as the polarized neutron studies reveal that this maximum is a property of the lattice. In this scenario the magnetic moment of all Yb ions would vary with temperature and the process of hybridization of the 4f electrons with the conduction electrons would be responsible for both observed maxima at $T = 130$ K and $T = 15$ K. Only the maximum at $T = 130$ K, the Curie–Weiss behaviour at higher temperatures and a temperature-independent enhanced Pauli susceptibility at low temperatures are described by the commonly used theoretical models. Whereas those models have been successfully used for many cerium and uranium compounds, a different temperature dependence of the ytterbium electronic level occupation, and/or an abrupt change in the density of states close to the Fermi level, as expected if the Fermi level is placed at (or *very* close) the Kondo resonance, might need to be considered for a sophisticated model for the ground state of $YbAl_3$.

Again, our present experimental situation does not allow us to distinguish between the two remaining possible scenarios (hypotheses (iii) and (iv)). In the first scenario (hypothesis (iii)), as the observed magnetization will depend on the concentration of the magnetic clusters, the observation of a low-temperature maximum would be sample dependent. In the second scenario (hypothesis (iv)) the observed maximum is independent of any impurity content. It would be interesting to study different $YbAl_3$ single crystals with polarized neutron diffraction and high-precision magnetization measurements. Moreover, as the Yb–Yb distance should be changed locally in clusters, it might be possible to prove the existence of magnetic clusters by analysing the x-ray absorption fine structure (XAFS).

4.2. Conduction electron polarization

The observed *temperature-independent* difference between the total and localized moment suggests a positive conduction electron polarization (CEP). Note that a form-factor deviation from a Yb^{3+} free ion would be observed at low scattering angles if the electrons in the outer shells, such as the 5d electrons of the Yb, were to be polarized. To analyse the CEP we point out that, in general, a Heisenberg-like magnetic interaction couples the conduction electrons ferromagnetically to the *spin* of the magnetic ion. Hence one expects a negative CEP with respect to the total moment for the light rare-earth elements with a less-than-half-filled 4f-electron shell, but a positive CEP for the heavy rare-earth elements. This has been observed for example in the $REAl_2$ (RE = Nd, Sm, Gd, Ho) series [25]. On the other hand, almost all Ce intermetallic compounds (especially those showing heavy-fermion or intermediate-valence behaviour) show an unusual positive CEP. Pavarini *et al* [26] have discussed this aspect of the form factor and concluded that a positive CEP in the case of cerium compounds is a consequence of hybridization. In our case the observation of a positive CEP in $YbAl_3$ is as expected for a heavy rare-earth element. Therefore in $YbAl_3$ the Yb ion cannot simply be described as the 'one-hole analogue' of cerium. It is worth noting that a 'sign inversion' of the CEP is not necessary for intermediate-valence or heavy-fermion behaviour, neither in the above-mentioned theory, nor from the experimental observation.

4.3. Comparison with $CeSn_3$

We conclude our discussion with a comparison of $YbAl_3$ with the isostructural and intermediate-valence compound $CeSn_3$ [27].

At first sight a surprising similarity appears in the temperature dependences of the magnetic susceptibilities of $YbAl_3$ and $CeSn_3$: a rapid increase of the magnetic susceptibility $\chi = \partial M/\partial B$ measured in low magnetic fields is observed for both compounds on lowering the

temperature. Nevertheless, a more careful look at this behaviour reveals important differences in the physical origins of those 'rising tails':

(a) First, no 'rising tails' have been observed for $YbAl_3$ in the 'high-field susceptibility' $\chi = M/B$ measured in strong magnetic fields, and therefore the 'rising tails' in the low-field susceptibility $\chi = \partial M/\partial B$ of $YbAl_3$ have been interpreted as being due to magnetic impurities, which are saturated in high fields. On the other hand, the magnetizations of the purest $CeSn_3$ samples increase linearly with applied field even at low temperatures and 'rising tails' in the 'high-field susceptibility' $\chi = M/B$ are therefore observed also in strong magnetic fields.

(b) Second, and even more important, at low temperatures and low scattering angles the observed form factor in $CeSn_3$ does *not* follow a Ce^{3+} free-ion form factor [28–30]. The data at higher scattering angles $\sin(\Theta)/\lambda > 0.2$ are well described by a Ce^{3+} free-ion form factor, which extrapolates for $Q = 0$ to a temperature-independent value of the 4f magnetic moment for all temperatures $T < 40$ K. The additional contribution observed in the form factor measurement at low temperatures ($T = 4$ K) and at low scattering angles ($\sin(\Theta)/\lambda < 0.2$) has been interpreted as a contribution due to a polarization of the Ce 5d electrons. This Ce 5d-electron polarization depends strongly on the stoichiometry of the sample and is maximal for the best (most stoichiometric) samples†. Hence it has been concluded that this temperature-dependent 5d-electron polarization is responsible for the intrinsic part of the 'rising tails' in the temperature dependence of the magnetic susceptibility.

On the other hand, the form factor of $YbAl_3$ is nicely described at all temperatures by a Yb^{3+} free-ion form factor, and it is the (linearly field-dependent) localized moment of the Yb^3 ion in the lattice which gives rise to the temperature dependence of the magnetic susceptibility, and especially to the second maximum observed at $T = 15$ K in addition to the one at $T = 130$ K. Note that no such second maximum has been observed for $CeSn_3$. As the Yb form factor remains unchanged even at small scattering angles, it might be concluded that the 4f–5d hybridization is smaller for Yb^{3+} than for Ce^{3+}, as is expected from the 4f-shell contraction along the lanthanide series.

Finally, we should point out that the CEP in $CeSn_3$ is positive as observed for many Ce compounds, but that this delocalized contribution to the total magnetization decreases with increasing temperature. Recall that the CEP in $YbAl_3$ is also positive but temperature independent to (at least) $T = 130$ K.

Acknowledgments

We thank E Brück, A Ivanov, G H Lander, A Murani and S M Shapiro for discussions. Support given to AH in the framework of the EC-funded training programme HCM is acknowledged.

References

[1] Brandt N B and Moshchalkov V V 1984 *Adv. Phys.* **33** 373
[2] Landelli A and Palenzona A 1972 *J. Less-Common Met.* **29** 293
[3] van Daal H J, van Aken P B and Buschow K H J 1974 *Phys. Lett.* A **49** 246
[4] Havinga E E, Buschow K H J and van Daal H J 1973 *Solid State Commun.* **13** 621
[5] Klaase J C P, Mattens W C M, de Boer F R and de Châtel P F 1977 *Physica* B **86–88** 234

† The modification of the form factor is maximal, whereas the susceptibility increases faster for the non-stoichiometric samples due to neighbouring phases such as Ce_2Sn_5.

[6] Majewski R E, Edelstein A S, Aldred A T and Dwight A E 1978 *J. Appl. Phys.* **49** 2096
[7] Klaase J C P, de Boer F R and de Chatel P F 1981 *Physica* B **106** 178
[8] Blyth R I R, Joyce J J, Arko A J, Canfield P C, Andrews A B, Fisk Z, Thompson J D, Bartlett R J, Riseborough P, Tang J and Lawrence J M 1993 *Phys. Rev.* B **48** 9497
[9] Patthey F, Imer J-M, Schneider W-D, Baer Y, Delley B and Hulliger F 1987 *Phys. Rev.* B **36** 7697
[10] Oh S-J, Suga S, Kakizaki A, Taniguchi M, Ishii T, Kang J-S, Allen J W, Gunnarsson O, Christensen N E, Fujimori A, Suzuki T, Kasuya T, Miyahara T, Kato H, Schönhammer K, Torikachvili M S and Maple M B 1988 *Phys. Rev.* B **37** 2861
[11] Imer J-M, Baer Y, Patthey F, Schneider W-D, Delley B and Hulliger F 1992 *Phys. Rev.* B **46** 1864
[12] Tjeng L H, Oh S-J, Cho E-J, Lin H-J, Chen C T, Gweon G-H, Park J-H, Allen J-W, Suzuki T, Makivic M S and Cox D L 1993 *Phys. Rev. Lett.* **71** 1419
[13] Cho E-J, Oh S-J, Olson C G, Kang J-S, Anderson R O, Liu L Z, Park J H and Allen J W 1993 *Physica* B **186+188** 70
[14] Murani A P 1985 *Phys. Rev. Lett.* **54** 1444
[15] Walter U, Holland-Moritz E and Fisk Z 1991 *Phys. Rev.* B **43** 320
[16] Murani A P 1994 *Phys. Rev.* B **50** 9882
[17] Shapiro S M 1996 private communication
[18] Hiess A, Boucherle J X, Givord F and Canfield P C 1995 *J. Alloys Compounds* **224** 33
[19] Hiess A, Boucherle J X, Givord F, Schweizer J, Lelièvre-Berna E, Tasset F, Gillon B and Canfield P C 1997 *Physica* B **234–236** 886
[20] Canfield P C and Fisk Z 1992 *Phil. Mag.* B **65** 1117
[21] Becker P J and Coppens P 1967 *Acta Crystallogr.* **23** 558
[22] Papoular R J and Gillon B 1990 *Neutron Scattering Data Analysis (Inst. Phys. Conf. Ser. 107)* (Bristol: Institute of Physics Publishing)
[23] Lander G H and Brun T O 1970 *J. Chem. Phys.* **53** 1387
[24] It is instructive to compare our findings for a paramagnetic system with the observation of magnetic spin waves in dilute magnetic systems such as Cu–Mn alloys; see
Lamelas F J, Werner S A, Shapiro S M and Mydosh J A 1995 *Phys. Rev.* B **51** 621
[25] Boucherle J X, Givord D and Schweizer J 1982 *J. Physique Coll.* **43** 199
[26] Pavarini E, Andreani L C and Amoretti G 1995 *Physica* B **206+207** 144
[27] Also, the linear coefficient of the specific heat is comparable with $\gamma \approx 60$ mJ K^{-2} mol^{-1}; see
Bonnet M, Boucherle J X, Givord F, Lapierre F, Lejay P, Odin J, Murani A P, Schweizer J and Stunault A 1994 *J. Magn. Magn. Mater.* **132** 289
[28] Stassis C, Loong C K, Harmon B N, Liu S H and Moon R M 1979 *J. Appl. Phys.* **50** 7567
[29] Boucherle J X, Fillion G, Flouquet J, Givord F, Lejay P and Schweizer J 1986 *J. Magn. Magn. Mater.* **54–57** 421
[30] Boucherle J X, Fillion G, Flouquet J, Givord F, Lejay P and Schweizer J 1986 *J. Magn. Magn. Mater.* **62** 277